APPLIED PHYSICS LETTERS VOLUME 80, NUMBER 3 21 JANUARY 2002

Study on the effect of plasma treatment on TiN films in N_2/H_2 atmosphere using x-ray reflectivity and secondary ion mass spectroscopy

S. Banerjee[a)]
LPEC, Faculté des Sciences, Université du Maine, Le Mans, France and Saha Institute of Nuclear Physics, 1/AF Bidhan Nagar, Calcutta 700064, India

A. Gibaud and D. Chateigner
LPEC, Faculté des Sciences, Université du Maine, Le Mans, France

S. Ferrari, C. Wiemer, and D. T. Dekadjevi
Lab. MDM-INFM via Olivetti 2, 20041 Agrate Brianza, Milano, Italy

(Received 3 July 2001; accepted for publication 9 November 2001)

We report the effect of plasma treatment on TiN films in N_2/H_2 atmosphere grown by chemical vapor deposition. The physical parameters and chemical evolution of the film as a function of duration of plasma treatment was studied using grazing incidence x-ray reflectivity (GIXR). From the analysis of GIXR we obtained the electron density profile of the film as a function of its depth. The GIXR data were analyzed using matrix method and distorted wave Born approximation scheme. Comparison of both the analysis schemes gives proper interpretation of the parameters obtained. The results obtained from the analysis of x-ray reflectivity data are supported by time of flight secondary ion mass spectroscopy depth profiling. © *2002 American Institute of Physics.*
[DOI: 10.1063/1.1435406]

TiN thin films are commonly used as diffusion barrier and adhesion layer in integrated circuit devices.[1] Recently, physical vapor deposition (PVD) for such kind of application was replaced by chemical vapor deposition (CVD), because of the increased conformality of the film as compared with PVD films.[2] The only drawback of the CVD film is that it shows an increased resistivity due to the inclusion of carbon impurities. The deposition is usually followed by a plasma treatment in N_2/H_2 atmosphere. The improvement of the TiN properties has been related to the reaction of N with Ti, resulting in more stoichiometric TiN, and the removal of carbon impurities due to reaction with hydrogen to form a volatile CH_4 gas. The effect of plasma on CVD TiN can be measured nondestructively by means of grazing incidence x-ray reflectivity (GIXR) technique.[3,4] From this technique one can obtain physical parameters such as the film thickness, density variation, evolution of interface roughness, and layer intermixing on plasma treatment applied to the system. In this present work we have used two formalisms to analyze the GIXR data, one based on model dependent matrix method[5–7] and the other a model independent method based on distorted wave Born approximation (DWBA).[8–11] We will discuss the importance of considering both the formalisms for the analysis and interpretation of the results. For supporting the analysis of the x-ray reflectivity data we have carried out time of flight secondary ion mass spectrometry (TOF-SIMS).

Ultrathin films of TiN have been deposited by metalorganic CVD from tetrakis-dimethylamino-titanium precursor on silicon wafers covered by native oxide. The deposition time was 10 s and a thickness of 100 Å is measured by ellipsometry. Sample A is the as deposited sample. Samples B–D underwent a plasma treatment in N_2/H_2 atmosphere at rf=750 W for 10, 20, and 40 s, respectively. Specular and off-specular x-ray reflectivity data were collected using laboratory x-ray source (Philips diffractometer) of wavelength 1.54 Å. The off-specular intensity from all samples was found to be very small, having values close to background count. TOF-SIMS depth profiles were collected by means of a dual beam ION-TOF CAMECA. We acquired negative ions generated by a Ga^+ at 25 keV primary source and using Cs^+ at energy of 1 keV for sputtering. TiN^- and C^- signals were chosen to observe the evolution of the film on the plasma treatment.

To calculate the x-ray reflectivity as a function of scattering vector Q_z, one requires l number of layers of thick-

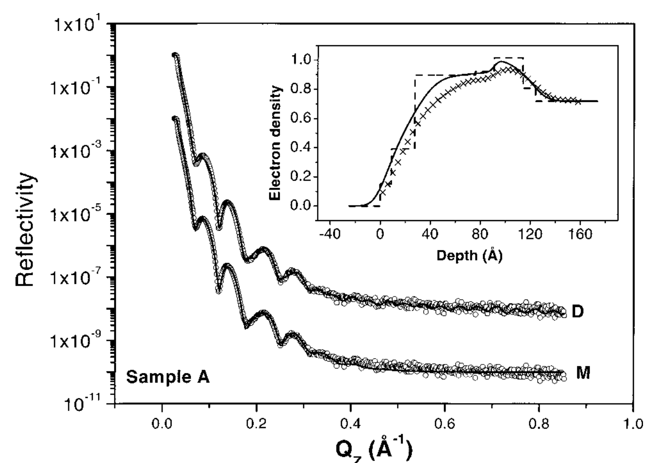

FIG. 1. Specular x-ray reflectivity data (○) for sample A and solid lines marked D and M are the curves obtained from DWBA and matrix method technique, respectively. Inset: EDP obtained from DWBA (×), matrix method (— — —), and convoluting the electron density value with the error function (_).

[a)]Electronic mail: sangam@cmp.saha.ernet.in

 © 2002 American Institute of Physics
Downloaded 21 Jan 2002 to 202.41.94.3. Redistribution subject to AIP license or copyright, see http://ojps.aip.org/aplo/aplcr.jsp

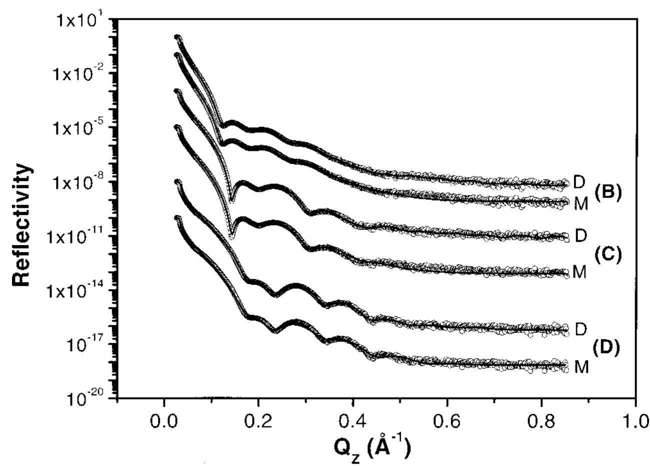

FIG. 2. Specular x-ray reflectivity data (○) for samples B, C, and D and solid lines marked D and M are the curves obtained from DWBA and matrix method, respectively.

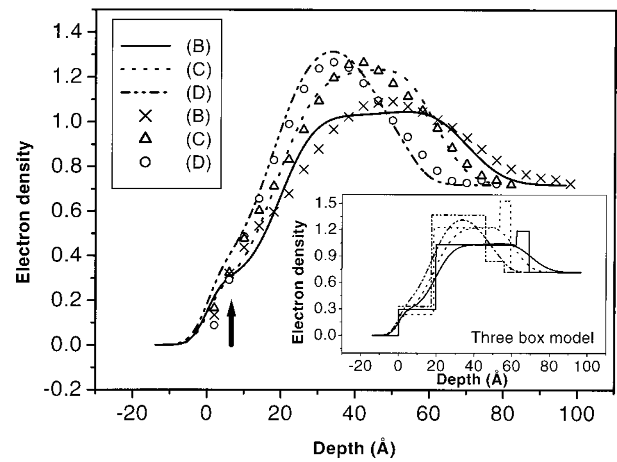

FIG. 3. EDP obtained from the DWBA (shown as symbols) and the matrix method (shown as lines) for samples B, C, and D. Inset: It shows the same EDP along with the electron density values as histograms to compare the EDP with the actual electron density value obtained from the matrix method for samples B (—), C (---), and D (–···–).

ness t_l. Each layer will have the electron density (ρ_l) and the electron density gradient "$(d\rho/dz)_l$" involved at each of the interfacial layers. If the electron density gradient $(d\rho/dz)_l$ has a Gaussian form then the reflectance coefficient at each of the interfaces is multiplied by a Debye–Waller factor like term, i.e., by $\exp(-Q_z^2\sigma_l^2/2)$ where σ_l is the full width at half maximum of the derivative of electron density $(d\rho/dz)_l$ of the lth layer. The abovementioned parameters $(t_l,\rho_l,(d\rho/dz)_l)$ can be adjusted by nonlinear least-square procedures so as to calculate the x-ray reflectivity using the matrix technique. Alternatively, for numerical calculations of x-ray reflectivity based on DWBA formalism, the total film is considered as a stack of many thin layers of equal thickness t. The lth slice at depth z ($z=lt$) has an electron density, $\rho_z=\rho_0+\Delta\rho_z$, where ρ_0 is an average electron density over the total film thickness and $\Delta\rho_z$ is a deviation of electron density from the average electron density as a function of depth z. Then the measured reflectivity intensities can be fitted to obtain the electron density profile (EDP) of the film, using $\Delta\rho_z$'s as fitting parameters.[8–10] The DWBA formalism was used to verify whether the EDP obtained by the matrix method, which is based on exact formalism, is meaningful. We will see below that the parameters obtained from the matrix method give higher values of ρ_l and σ_l but when they are convoluted to obtain the EDP then one gets electron density values similar to DWBA.

In Fig. 1 we have shown the x-ray reflectivity data of plasma untreated sample A. The best reflectivity fit is shown as a solid line and is labeled as M for the fit obtained using six boxes by matrix method and labeled as D for the fit obtained by the DWBA formalism (Note: The number of boxes considered in the matrix method does not mean that the film consists of that many layers. It only provides a model to obtain the EDP of the film.) In the inset of Fig. 1 we show the electron density values for each of the layers as an histogram (dashed line). The EDP is easily derived from the fit parameters. Since dρ/dz at each interface was considered to have a Gaussian form, the EDP $\rho(z)$, is represented by a series of error functions shown as a solid line in the inset of Fig. 1. In the case of the DWBA method, the thickness of each layer was fixed to 4 Å and 40, 25, 21, 20 numbers of layers were considered resulting in 156, 96, 80 and 76 Å for samples A–D, respectively, as the total range of analysis. One generally takes in this scheme the range larger than the nominal total thickness of the film to make sure that some portion of the substrate is included in the analysis. The EDP which is obtained in this calculation does not depend on *a priori* model of the film and is therefore model independent. The EDP obtained by this formalism is shown as symbols in the inset of Fig. 1. We observe from the inset of Fig. 1 that the EDP obtained from the matrix method and that from the DWBA formalism more or less fall on each other.

In Fig. 2 we show the reflectivity data for samples B, C, and D. The best fit obtained with each formalism is shown as a solid line. For the matrix method we could obtain the best fit using only three boxes. The convoluted EDPs obtained by the matrix method and the EDP obtained from the DWBA formalism are shown in Fig. 3. The values of the fit param-

TABLE I. Parameters obtained from the matrix method, $\mathbf{Q}_c$(Å^{-1}), σ(Å), and $\mathbf{t}_l$(Å)[$\mathbf{Q}_c/\sigma/\mathbf{t}_l$], where $\mathbf{Q}_c=0.0375\sqrt{\rho}$ (see Ref. 7).

	Sample A	Sample B	Sample C	Sample D
Substrate	0.0318/7.4/∞	0.0318/8.5/∞	0.0318/7.7/∞	0.0318/4.0/∞
Layer 1	0.0337/13.4/9.9	0.0409/10.5/6.6	0.0465/7.0/5.7	0.0344/7.7/10.0
Layer 2	0.0378/3.4/23.1	0.0382/7.2/42.8	0.0415/8.6/34.8	0.0440/8.4/28.5
Layer 3	0.0368/11.1/15.1	0.0204/3.4/19.7	0.0184/3.2/18.6	0.0215/3.6/17.4
Layer 4	0.0355/14.7/48.3	⋯	⋯	⋯
Layer 5	0.0235/8.2/18.6	⋯	⋯	⋯
Layer 6	0.0147/6.6/9.0	⋯	⋯	⋯

Downloaded 21 Jan 2002 to 202.41.94.3. Redistribution subject to AIP license or copyright, see http://ojps.aip.org/aplo/aplcr.jsp

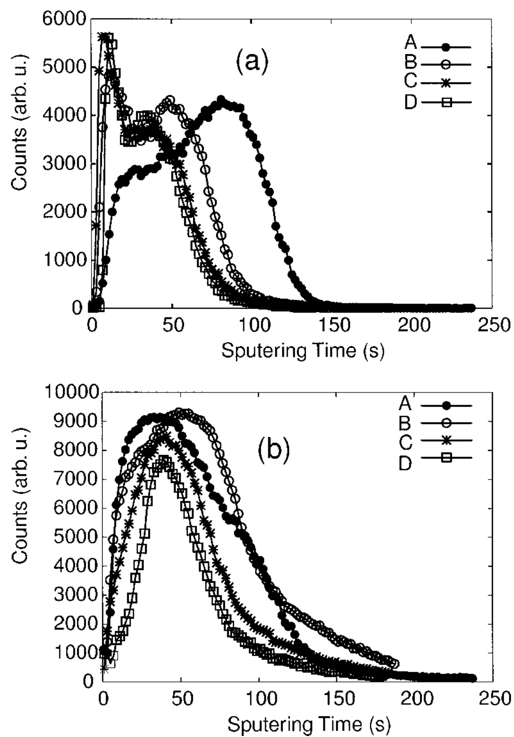

FIG. 4. TOF-SIMS depth profiles of TiN films. (a) TiN^- and (b) C^- profile for samples A through D.

eters for the matrix method are tabulated in Table I. In the inset of Fig. 3, we show the respective electron densities ρ_l of each of the layers as histograms and the convoluted EDP $\rho(z)$ obtained by the matrix method. We observe that for all the samples the EDP obtained by the matrix and DWBA method are similar. At a closer look in the inset of Fig. 3 one can see from the histograms that the samples B and C exhibit larger values of the electron density for the layer adjacent to the substrate. The convolution with the error functional form, whose width is determined by the value of σ, results in the lowering of the electron density. This is a direct consequence of a large value of σ obtained from the fit. We would like to stress here that the EDP obtained after the convolution is a more meaningful quantity than just the electron density value for each of the layers. It is interesting to point out that σ values can be of the order or even greater than the layer thickness as can be seen from Table I.

From Figs. 1 and 3 we observe that the film thickness for sample A is ~125 Å and with the plasma treatment the thickness of the film is reduced to ~80 Å, ~70 Å, and ~60 Å for samples) B, C, and D, respectively. These values are obtained from the position of the depth where the value of the electron density approaches the value of the Si substrate. The air/film and film/substrate interfaces are not very sharp and the interface can be considered to be diffuse. We also observe that the electron density of the film increases with the plasma processing. The reduction of the film thickness as a function of plasma processing is due to the plasma etching. The carbon present in CVD film gives rise to complex polymeric structures of low density with embedded TiN clusters. The removal of carbon during plasma treatment causes TiN clusters to form a compact TiN film resulting in an increase in the electron density. To support the analysis of x-ray reflectivity, we have carried out TOF-SIMS. Figure 4(a) shows TiN^- profile for samples A through D and we observe that the plasma treatment is causing a decrease in the film thickness. We observe that for the sample A the TiN^- profile obtained from SIMS is similar to the EDP as shown in the inset of Fig. 1. We also observe the formation of a compact TiN layer at the surface for the plasma treated films and is apparent by the maximum in TiN^- intensity at the beginning of the profile for samples B, C, and D. Taking a closer look at the EDP of samples A through D we observe a shoulder around 10 Å depth for the plasma treated samples (shown by an arrow mark in Fig. 3) which is not seen for the untreated sample A. The presence of the shoulder can be correlated to the observed maximum in the TiN^- intensity at the beginning of the SIMS profile for all plasma treated samples. The replacement process of C by N is efficient only in the superficial part of the film, whereas in the bulk, high amount of carbon is retained. In Fig. 4(b) are shown C^- profiles for samples A through D. We observe that at the surface of the film the carbon signal is drastically reduced, while in the middle of the film carbon is reduced only slightly. The replacement of C by N gives rise to an increase of electron density as also obtained from the analysis of x-ray reflectivity. The electron density obtained from the x-ray reflectivity is indeed well explained by the chemical observation made with SIMS.

In conclusion, we have observed from the analysis of x-ray reflectivity and TOF-SIMS a decrease in the thickness of TiN films as the plasma processing continues for a longer time. As the plasma processing time increases, we observe an increase of the electron density of the TiN film which has been attributed to the substitution of C by N. The whole process of plasma treatment can be followed using nondestructive GIXR technique in conjunction with SIMS.

[1] M. Danek, M. Liao, J. Tseng, K. Littau, D. Saigal, H. Zhang, R. Mosely, and M. Eizenberg, Appl. Phys. Lett. **68**, 1015 (1996).
[2] H.-L. Chang and P.-R. Jeng, Jpn. J. Appl. Phys., Part 1 **39**, 4738 (2000).
[3] L. G. Parratt, Phys. Rev. **95**, 359 (1954).
[4] S. Banerjee, A. Datta, and M. K. Sanyal, Vacuum **60**, 371 (2001).
[5] M. Born and E. Wolf, *Principles of Optics*, 6th ed. (Pergamon, London, 1980).
[6] B. Vidal and P. Vincent, Appl. Opt. **23**, 1794 (1984).
[7] A. Gibaud, *X-Ray and Neutron Reflectivity: Principles and Applications* (Springer, Berlin, 1999), Chap. 3, p. 87.
[8] M. K. Sanyal, J. K. Basu, A. Datta, and S. Banerjee, Europhys. Lett. **36**, 265 (1996).
[9] S. Banerjee, M. K. Sanyal, A. Datta, S. Kanakaraju, and S. Mohan, Phys. Rev. B **54**, 16377 (1996).
[10] S. Banerjee, Y. J. Park, D. R. Lee, Y. H. Jeong, K.-B. Lee, S. B. Yoon, H. M. Choi, J. C. Park, J. S. Roh, and M. K. Sanyal, Appl. Surf. Sci. **136**, 41 (1998).
[11] X. L. Zhou and S. H. Chen, Phys. Rep. **257**, 223 (1995).

Downloaded 21 Jan 2002 to 202.41.94.3. Redistribution subject to AIP license or copyright, see http://ojps.aip.org/aplo/aplcr.jsp